

Research paper

Alteration of organ size and allometric scaling by organ-specific targeting of IGF signaling

Hiroyasu Kamei ^{a,*}, Cunming Duan ^b^a Faculty of Biological Science and Technology, Institute of Science and Engineering, Kanazawa University 11-4-1, Ossaka, Noto, Ishikawa 927-0552, Japan^b Department of Molecular, Cellular, and Developmental Biology, University of Michigan, Ann Arbor, MI 48109-1048, United States

ARTICLE INFO

Keywords:

Insulin-like growth factor binding protein
Insulin-like growth factor 1 receptor
Akt
Organ growth
Eye
Heart

ABSTRACT

The size of an organ is proportional to the other body parts or the whole body. This relationship is known as allometry. Understanding how allometry is determined is a fundamental question in biology. Here we tested the hypothesis that local insulin-like growth factor (Igf) signaling is critical in regulating organ size and its allometric scaling by organ-specific expression of Igf binding protein (Igfbp). Overexpression of Igfbp2a or 5b in the developing zebrafish eye, heart, and inner ear resulted in a disproportional reduction in their growth relative to the body. Stable transgenic zebrafish with lens-specific Igfbp5b expression selectively reduced adult eye size. The action is Igf-dependent because an Igf-binding deficient Igfbp5b mutant had no effect. Targeted expression of a dominant-negative Igf1 receptor (dnIgf1r) in the lens caused a similar reduction in relative eye growth. Furthermore, co-expression of IGF-1 with an Igfbp restored the eye size. Finally, co-expression of a constitutively active form of Akt with Igfbp or dnIgf1r restored the relative eye growth. These data suggest that local Igf availability and Igf signaling activity are critical determinants of organ size and allometric scaling in zebrafish.

1. Introduction

In multicellular organisms, the size of each organ grows proportional to other organs and to the entire body. This morphological scaling relationship is known as allometry (Frankino et al., 2019; Vea and Shingleton, 2020). Understanding how allometry arises is a fundamental question in biology. To date, invertebrate models with diverse morphological features have been instrumental in our understanding of allometry regulation (Mirth et al., 2016). An emerging theme is that nutrient-sensitive insulin-like peptides (ILPs) play critical roles in allometric scaling (Texada et al., 2020). For instance, imaginal discs (primordia of the adult organ) of the genital arch of the fruit fly, *Drosophila melanogaster*, and the male sexual ornaments, or horn, of rhinoceros beetle, *Trypoxylus dichotomus*, have different sensitivity to ILPs compare to the other body parts, which contributes to the unique allometric scaling of these organs (Emlen et al., 2012; Shingleton et al., 2005; Tang et al., 2011). An organ possessing elevated sensitivity to ILPs has a greater growth rate and achieves a larger final size relative to the other body parts.

In the vertebrates, the ancestral insulin-like gene has evolved into insulin, IGF-1, IGF-2, and ILPs, including relaxin and several relaxin-like

peptides (Lu et al., 2005; Wood et al., 2005a). Insulin and IGFs, in particular, are implicated in somatic growth and metabolism (Wood et al., 2005a). While insulin acts via the insulin receptor, IGF-1 and IGF-2 act via the type1 IGF receptor (IGF1R) (Duan et al., 2010; Duan and Xu, 2005). The intracellular signaling cascades downstream of the insulin receptor and the IGF1R are largely overlapping, including protein kinase B (Akt), the target of Rapamycin, and mitogen-activated protein kinase (Duan et al., 2010; Duan and Xu, 2005). Insulin is predominantly secreted from pancreatic β -cells and act as an endocrine factor. Unlike insulin, however, IGF-1 and IGF-2 are not only produced and secreted from the liver, but also expressed in many, if not all, other tissues. Therefore, they act as endocrine, paracrine, and autocrine factors. However, the precise roles of the systemic (endocrine) and local (paracrine and/or autocrine) IGF actions in allometry regulation are not well understood.

IGFs, but not insulin, are bound to a family of high-affinity IGF binding proteins (IGFBPs/Igfbps) in extracellular environments (Allard and Duan, 2018; Clemons, 2012, 2016; Firth and Baxter, 2002). These IGFBPs prevent the potential binding of circulating IGFs to the insulin receptor and therefore segregate the two hormonal system (Clemons, 2012, 2016; Firth and Baxter, 2002). Functional studies suggest that

* Corresponding author.

E-mail address: hkamei@se.kanazawa-u.ac.jp (H. Kamei).

these IGFBPs/Igfbps can bind to IGFs with an affinity equal to or even greater than the IGF1R and they can modulate IGF biological activity by regulating IGFs available to the IGF1R. There are six types of IGFBPs, designated IGFBP-1 through IGFBP-6. Humans and other mammals have one gene belonging to each of the six IGFBP types (Allard and Duan, 2018). Due to a teleost lineage specific genome duplication event, teleost fish generally have more Igfbps (Allard and Duan, 2018). It is now clear that Zebrafish has 9 *igfbp* genes, including 2 *igfbp1*, 2 *igfbp2*, 1 *igfbp3*, 2 *igfbp5*, and 2 *igfbp6* genes. All these 9 *igfbp* genes have been characterized and their spatiotemporal expression patterns studied to various degrees (Dai et al., 2010; Duan et al., 1999; Kajimura et al., 2005; Kamei et al., 2008; Li et al., 2005; Maures and Duan, 2002; Wang et al., 2009; Wood et al., 2005b; Zhou et al., 2008). Among them, *igfbp1a* and *igfbp1b* genes are highly expressed in the liver in response to hypoxia, starvation, and chronic stresses (Kajimura et al., 2005; Kamei et al., 2008; Maures and Duan, 2002). The *igfbp2a* mRNA is detected in the lens and in brain boundary vasculature during embryogenesis. Subsequently it becomes highly expressed in the liver (Wood et al., 2005b; Zhou et al., 2008). The paralogous *igfbp2b*, on the other hand, is initially expressed in all tissues at low levels, but later becomes abundant in the liver (Zhou et al., 2008). In comparison, *igfbp3* mRNA is first detected in the cranial neural crest cells and subsequently in pharyngeal arches and inner ears (Li et al., 2005). During early development, *igfbp5b* mRNA was transiently expressed in differentiating somites, gill arches, pectoral fin, and neural tissues. In comparison, *igfbp5a* mRNA is highly expressed in ionocytes located in the yolk sac region and subsequently in the gills (Dai et al., 2010; Liu et al., 2018). The *igfbp6* mRNA levels were relatively low during embryogenesis (Wang et al., 2009).

The goal of this study is to investigate the role of local Igf signaling in organ size and allometric scaling by targeted overexpression of Igfbps. We chose to express Igfbp2a and Igfbp5b because they were well characterized and reagents are ready available (Dai et al., 2010; Duan et al., 1999; Liu et al., 2018; Wood et al., 2005b). Overexpression or addition of exogenous Igfbp2a and Igfbp5b inhibits IGF actions (Dai et al., 2010; Duan et al., 1999; Liu et al., 2018; Zhou et al., 2008). Zebrafish is a suitable vertebrate model to test the role of local Igf signaling in allometry regulation due to its fast growth and development, free-living embryos, the availability of many genetic tools such as tissue-specific promoters and the Tol2 transposon-mediated transgenesis (Kawakami, 2004). Importantly, the zebrafish Igf-Igfbps are well characterized, and they are highly similar to mammals (Allard and Duan, 2018; Duan and Allard, 2020).

2. Materials and methods

2.1. Chemicals

RNase-free DNase and restriction enzymes were purchased from Promega (Madison, WI). High-fidelity DNA polymerase (*PfuUltra*™) was purchased from Stratagene (La Jolla, CA). All oligonucleotide primers were purchased from Invitrogen Life Technologies, Inc. (Carlsbad, CA). All other chemicals were reagent grade and purchased from Fisher Scientific (Pittsburgh, PA) unless otherwise noted.

2.2. Experimental animals

Adult zebrafish (*Danio rerio*) were maintained at 28 °C on a 14 h:10 h (light: dark) cycle and fed twice daily. Embryos were generated from natural crosses, and the fertilized eggs were raised at 28.5 °C and staged according to a previous report (Kimmel et al., 1995). All experiments were conducted under guidelines approved by the University Committee on the Use and Care of Animals, University of Michigan at Ann Arbor.

2.3. Lens-, heart-, and otic vesicle-specific gene promoters

We chose to express *igfbps* in the eyes, heart, and inner ear because

these organ shapes are relatively easy to measure and the promoter constructs, antibodies, and marker genes are readily available. Zebrafish α -A-crystallin gene (α Acry) promoter DNA (2.8 k bp) was used for targeting transgene expression in the lens. The α Acry promoter DNA was kindly provided by Dr. Sumiko Watanabe, The University of Tokyo (Kurita et al., 2003). To express a transgene in the heart, a 259 bp DNA fragment encoding the minimum promoter sequence of the cardiac myosin light chain-2 gene (*cmlc2*) was cloned and used following a previous report (Huang et al., 2003). The *cmlc2* promoter DNA was cloned using the *PfuUltra*™ DNA polymerase and the following primers: 5'-TTTGATTCATTTCATCCCTCAAATCTCTCATTCACGTC-3' and 5'-TTGGATCCTCACTGTCTGCTTGGTCTGGGCT-3'. For targeting transgene expression in the otic vesicles, a 2.2 k bp DNA fragment encoding the promoter sequence of zebrafish otolith-matrix protein-1 gene (*omp1*) was cloned using the *PfuUltra*™ DNA polymerase and the following primers: 5'-TCCTATTAAATGGCCATGTCATTTCTATGGGAA-3'; 5'-TCCTCTGGAGGTTGCTTTAACAGTAACCTTC-3'. All DNA constructs were sequenced.

2.4. Construction of organ-specific gene expression vectors

Two types of expression constructs were generated and used for targeting transgene expression in the developing lens. In the first, the α Acry promoter DNA was subcloned into the pEGFP-N1 or pEYFP-N1 vector (Invitrogen, Carlsbad, CA) by replacing the original cytomegalovirus promoter using suitable restriction enzymes. Next, cDNA of zebrafish Igfbp2a or Igfbp5b coding sequence lacking the stop codon was placed between the α Acry promoter and EGFP/EYFP using BspHI/NcoI-NotI or NcoI site, resulting in an Igfbp-GFP/YFP fusion protein (Supplemental Fig. S1A). In the second type, an internal ribosomal entry site sequence (IRES) was inserted between the Igfbp and EGFP/EYFP sequences to allow the simultaneous expression of the Igfbp and EGFP/EYFP. This was because adding a GFP tag in zebrafish Igfbp3 can affect its IGF binding property (Zhong et al., 2011). In addition, the transposon-mediated gene integration system (Tol2-system) (Kawakami, 2004) was used to increase the transgenesis efficiency (Supplemental Fig. S1B). To target Igf signaling in the heart, the *cmlc2* promoter cDNA was subcloned into EYFP-N1 vector by replacing the original cytomegalovirus promoter using suitable restriction enzymes. Next, cDNA encoding Igfbp2a lacking the stop codon was placed between the promoter and YFP using BamHI-AgeI sites to generate the heart-specific Igfbp2a-YFP expression vector (Supplemental Fig. S1C). The inner ear expression construct was engineered using a similar manner. But an IRES was between the Igfbp5b and EYFP sequence and Tol2 sites were added (Supplemental Fig. S1D).

2.5. Microinjection

Plasmid DNA was purified using the endotoxin-free DNA extraction system (UltraClean Endotoxin Free Mini Plasmid Prep Kit, MO BIO Laboratories, Inc., Carlsbad, CA) according to the manufacturer's instruction. The 25 ng mL⁻¹ DNA solution was prepared, and 4 nL of the solution (100 pg of DNA) was injected into 1-cell stage zebrafish embryos as described previously (Kamei et al., 2011). When the transposon vector was injected, 75 pg transposase RNA was co-injected with the Tol2-based plasmid for efficient DNA delivery to the fish genome. The injected embryos were raised to various stages. Successful transgene expression was confirmed under a fluorescence microscope and changes in relative organ size were determined as described below.

2.6. Germ-line transgenesis

Embryos injected with the Tol2 DNA vector (pT2- α Acry:igfbp5b:IRES:YFP) and the transposase RNA were raised to adulthood. The F0 fish were intercrossed to generate F1 fish. F1 fish were screened by lens-specific YFP fluorescence. The selected F1 fish were intercrossed to

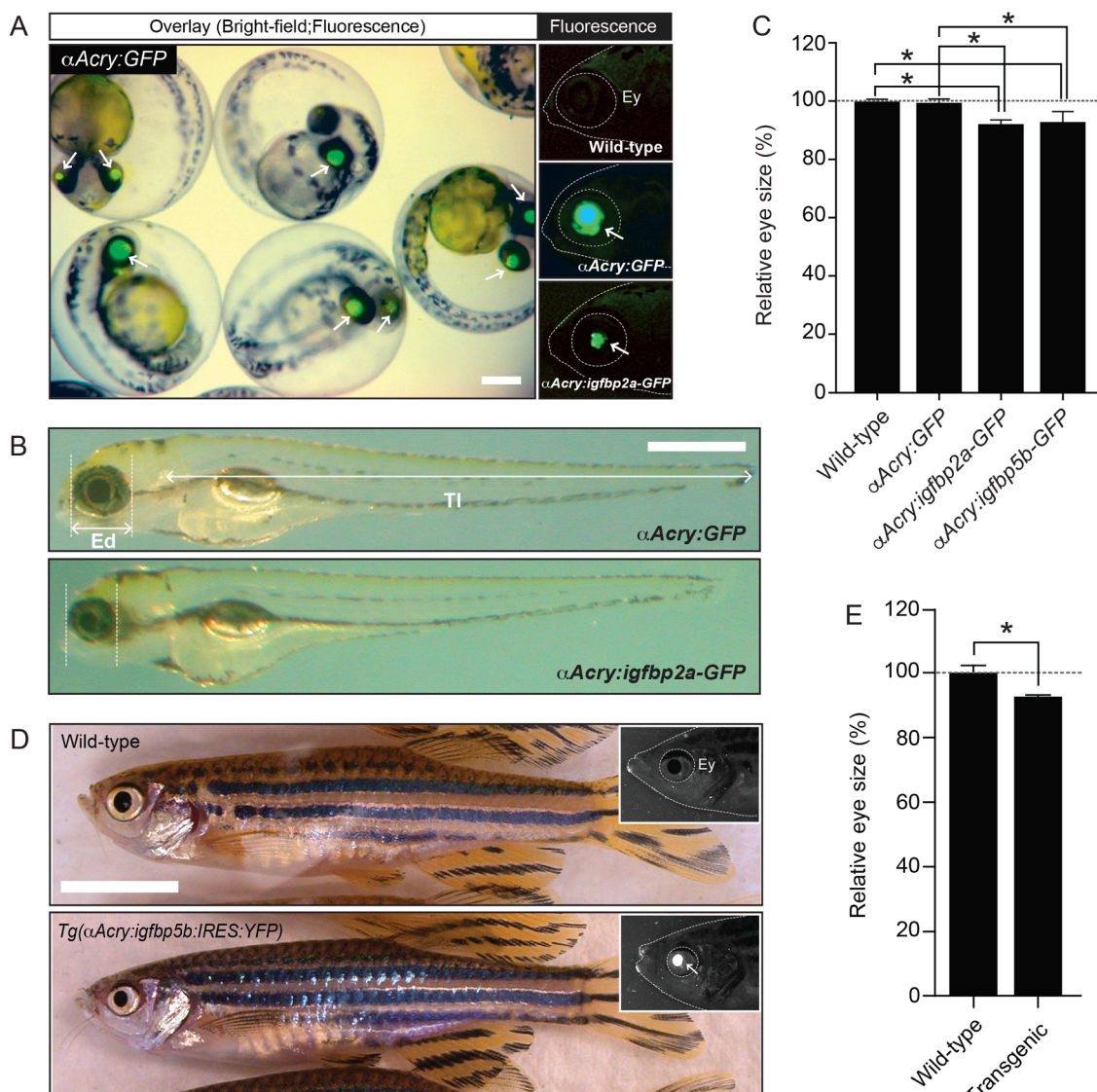


Fig. 1. Targeted expression of Igfbps in the lens reduces relative eye size. (A) Representative images of 2 dpf zebrafish embryos injected with the indicated expression vectors (left column). In the fluorescent images (right column), the head and eye in a 6 dpf are outlined by dotted lines. Arrows indicate the lens-specific GFP signal. Scale bar = 250 μ m. (B) Representative images of 4 dpf larvae injected with the indicated expression vectors. Scale bar = 500 μ m. Ed (Eye-diameter) and Tl (trunk-length) are indicated. (C) Relative eye size of 5 dpf larvae fish with the indicated transgene expression. $n = 5-16$. *, $P < 0.05$. (D) Representative image of 7 month old wild-type and *Tg(αAcry:igfbp5b:IRES:YFP)* fish. Scale bar = 1.0 cm. The inset images show lens-specific YFP signal (arrow) in *Tg(αAcry:igfbp5b:IRES:YFP)* fish. (E) Relative eye size of adult wild-type and *Tg(αAcry:igfbp5b:IRES:YFP)* fish. $n = 5$. *, $P < 0.05$.

generate F2 fish. F2 fish were raised to adulthood.

2.7. Relative organ size measurement

The average eye diameter (Ed: averages of the left and right eye diameters) and the trunk length (Tl: length from the center of the ear to end of the trunk excluding the caudal fin) were measured. The relative eye size is calculated by dividing the Ed value with Tl. The effect of Igfbp2a overexpression in the eye size was evident at least 7 days post fertilization (dpf). Therefore, the measurement of relative eye size was carried at 4, 5, and 6 dpf depending on the spawning day in the week. The sizes of heart and inner ear were measured at 77 and 60 h post fertilization (hpf) respectively because of the developing timing of the organogenesis and the timing of the transgene expression. To determine the heart size, embryos were stained with the MF20 antibody (Developmental studies hybridoma bank, University of Iowa, IA). The stained embryos were imaged from the ventral view. The ventricle size was

measured based on the outline tracing. The value was divided by Tl, resulting in the relative heart size. The otic vesicle size was measured by tracing its outline in the lateral view. The relative otic vesicle or inner ear size was calculated by dividing the value of the measured area with the Tl value. The final relative organ size value in each experimental group was calculated and presented as % of the control group value. All these measurements were conducted using the ImageJ/Fiji software (NIH, Bethesda, MD).

2.8. Whole-mount immunohistochemistry

Embryos were fixed with 4% paraformaldehyde in phosphate-buffered saline not containing Ca^{2+} and Mg^{2+} ions (PBS(-) for 3 hrs at room temperature or 6 hrs overnight at 4 °C. The samples were washed and permeabilized. They were washed with tris-buffered saline (TBS) and incubated with the TBST solution (1% bovine serum albumin; 1% dimethyl sulfoxide; 0.1% Triton-X100 in TBS) containing 2% normal

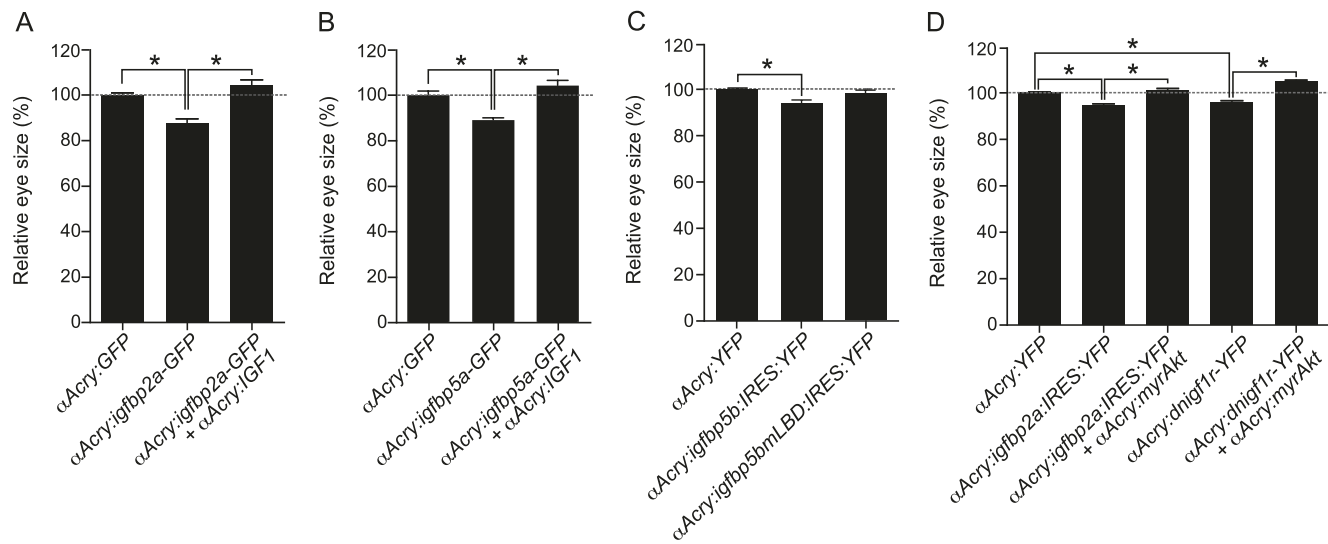


Fig. 2. The action of Igfbps in relative organ size is Igf binding- and Igf1r signaling-dependent. (A) Relative eye size of 5 dpf fish with the indicated transgene expression. $n = 14-54$. *, $P < 0.05$. (B) Relative eye size of 6 dpf fish with the indicated transgene expression. $n = 10-21$. *, $P < 0.05$. (C) Relative eye size of 4 dpf fish with the indicated transgene expression. Igfbp5bmlLBD, Igfbp5b ligand-binding deficient mutant. $n = 8-19$, *, $P < 0.05$. (D) Relative eye size of 4 dpf fish with the indicated transgene expression. dnlIgf1r, dominant-negative Igf1 receptor. myrAkt, myristoylated Akt. $n = 24-64$. *, $P < 0.05$.

goat serum to block non-specific binding sites for 1hr at room temperature. The samples were then incubated with the MF20 antibody diluted as 1: 25 in the blocking solution overnight at 4 °C. After a series of washing in TBST, they were treated with secondary antibody (anti-rabbit IgG-Cy3, 1: 800) in TBST overnight at 4 °C.

2.9. Statistics

Values are shown as mean \pm SEM. The Student's *t*-test was used for two-group comparisons. The statistical significance among multiple groups was determined by one-way analysis of variance (ANOVA) followed by Fisher's least significant difference test. Statistical tests were performed by GraphPad Prism 7.0 software (GraphPad, San Diego, CA), and the significance was recognized at $P < 0.05$.

3. Results and discussion

3.1. Targeted expression of Igfbps in the lens reduces relative eye size and allometry

We used the α Acry promoter, which drives the transgene expression in the lens (Kurita et al., 2003), to target the local Igf signaling in the developing eyes. As previously reported (Kurita et al., 2003), the α Acry promoter drove GFP expression exclusively in the lens. The GFP signal was detected beginning at 28–32 hpf, and continued at least until 6 dpf (Fig. 1A). Approximately $84.6 \pm 8.3\%$ of the α Acry:GFP DNA injected embryos showed GFP signal in the lens at 6 dpf, indicating a high penetrance. Next, Igfbp2a-GFP and Igfbp5b-GFP were targeted expressed in the lens using the α Acry promoter (Supplemental Fig. S1A). The expression of Igfbp2a-GFP and Igfbp5b-GFP was confirmed (Fig. 1A, Supplemental Fig. S2). As shown in Fig. 1B, the relative eye size in the Igfbp2a-GFP group was significantly smaller compared with that of the wild-type or GFP-expressing control fish (Fig. 1B and 1C). Likewise, targeted expression of Igfbp5b-GFP resulted in a similar reduction in the relative eye size at 5 dpf (Fig. 1C). It has been previously reported that GFP tagging of zebrafish Igfbp3 can affect its IGF binding property (Zhong et al., 2011). Among the IGFBPs/Igfbps, IGFBP3/Igfbp3 is most closely related to IGFBP3/Igfbp3 (Allard and Duan, 2018). To ascertain that expression of an native Igfbp indeed affects eye growth, we generated pT2- α Acry:igfbp:IRES:YFP expression constructs, in which an IRES was added to allow the simultaneous expression of the Igfbp and

YFP proteins. In addition, Tol2 sites were added to increase the transgenesis efficiency (Supplemental Fig. S1B). These constructs successfully targeted transgene expression in the lens (Supplemental Fig. S2B). Transient expression of Igfbp2a or Igfbp5b in the lens reduced the relative eye size in larval fish at 5 and 7 dpf (Fig. 2C and 2D; Supplemental Fig. S3), but this effect was not significant in the juvenile fish (Supplemental Fig. S3). These results suggest that transient overexpression of Igfbp2a or Igfbp5b in the lens resulted in a disproportional reduction in eye growth relative to the body.

To determine whether targeting Igf signaling by overexpressing an Igfbp affects adult eye size, *Tg(αAcry:igfbp5b:IRES:YFP)* fish, a transgenic zebrafish line in which Igfbp5b is stably expressing in the lens, was generated and used for morphometric analysis (Fig. 1D). The relative eye size in adult *Tg(αAcry:igfbp5b:IRES:YFP)* fish was significantly smaller than that of the wild-type fish (Fig. 1E), suggesting that stable expression of an Igfbp5b alters the allometric scaling in adult fish.

3.2. Igfbp expression alters organ size by changing IGF bioavailability and reducing Igf1r signaling

IGFBPs/Igfbps have been shown to have IGF-dependent and independent actions (Allard and Duan, 2018). If the Igfbps decrease eye growth by binding to local Igfs and sequestering them from binding to the Igf1r, then overexpressing an Igf ligand should reverse this effect. This idea was tested by transient co-expression of Igfbp2a-GFP or Igfbp5a-GFP with human IGF-1. Indeed, the eye size reduction caused by Igfbp2a-GFP or Igfbp5a-GFP expression was alleviated by IGF-1 co-expression (Fig. 2A and B). To determine that the effects of Igfbp expression are indeed Igf-dependent, we compared the activity of Igfbp5b with its ligand-binding deficient mutant, Igfbp5bmlLBD, which has impaired IGF binding capability (Dai et al., 2010) by transient transgenic experiments. While the expression of Igfbp5b in the lens resulted in a significant decrease in the relative eye size, Igfbp5bmlLBD did not have such effects (Fig. 2C), suggesting this action of Igfbp5b requires IGF binding. The expression of the transgene was confirmed by YFP signal (Fig. S2B).

To test the role of local IGF signaling further, a dominant-negative form of zebrafish Igf1r (*dnlIgf1r*) was transiently expressed in the lens. Previous studies showed that expression of the *dnlIgf1r* inhibited Igf1r-mediated Akt signaling in zebrafish embryos (Kamei et al., 2011; Onuma et al., 2011). As shown in Fig. 2D, expression of the *dnlIgf1r*

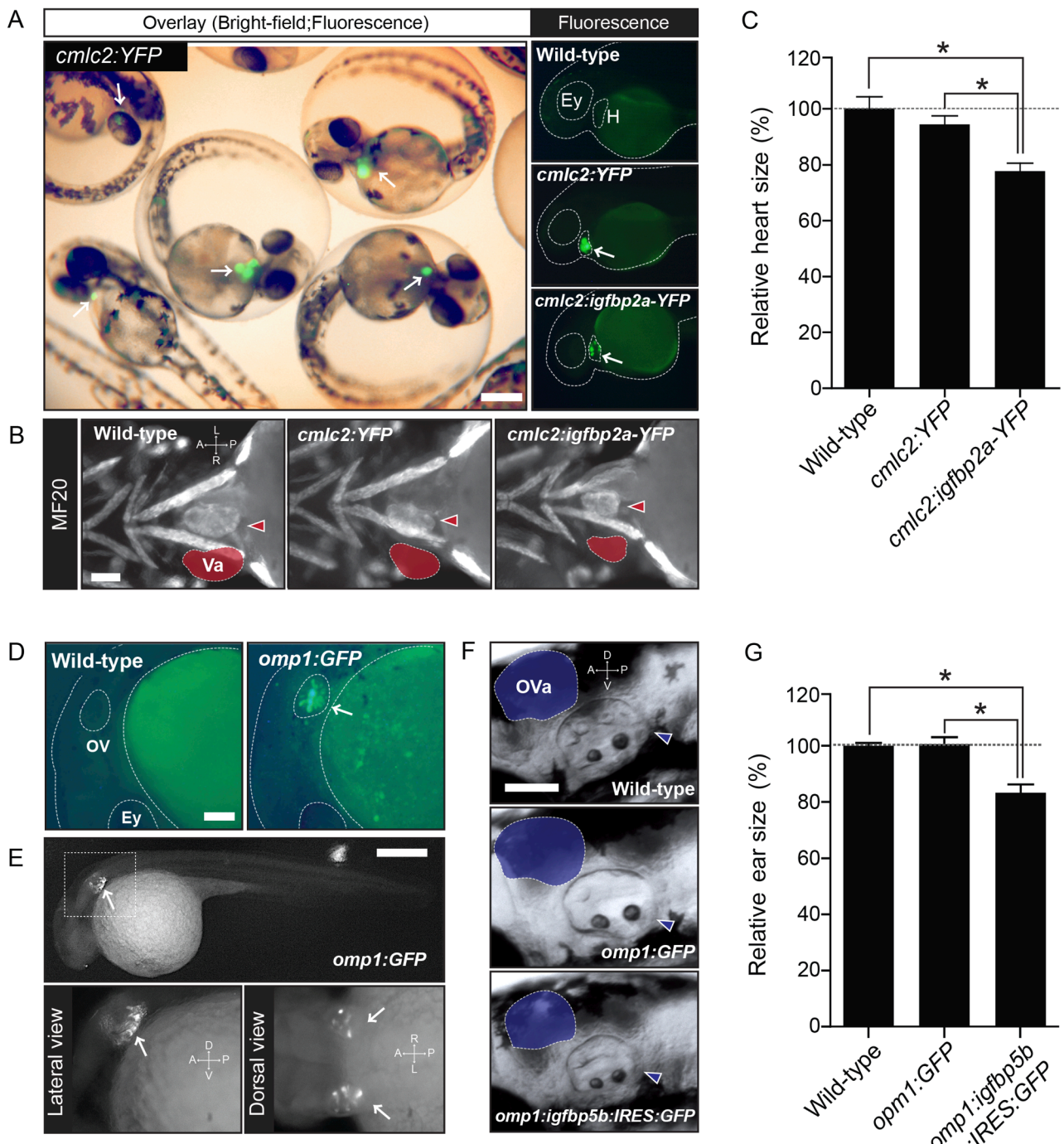


Fig. 3. Targeted expression of an Igfbp in the heart and inner ear reduces relative heart and inner ear size. (A) Representative images of 60 hpf (left panel: overlay image) and 72 hpf (right panels) zebrafish larvae injected with the indicated expression vectors. In the fluorescent images (right column), the eye (Ey), heart (H), and body are outlined by dotted lines. Arrows indicate the heart-specific YFP signal. Scale bar = 250 μ m. (B) Representative images of 77 hpf larvae stained with MF20 to visualize the ventricle. Red arrowhead points to the ventricle. The ventricle area (Va) was traced (marked by red color) and measured as described in the Materials and Methods. Scale bar = 50 μ m. (C) Relative heart size in 77 hpf larvae of the indicated group. $n = 16-24$. *, $P < 0.05$. (D) Representative images of 24 hpf embryos injected with the indicated expression constructs. The outline of the embryo, eye (Ey), and otic vesicle (OV) is marked by dotted lines. Scale bar = 100 μ m. (E) Representative image of a 32 hpf *omp1:GFP* embryo. Scale bar = 250 μ m. (F) Representative images of 60 hpf larvae. OV is indicated by an arrowhead. The area of OV (Ova) is presented graphically as a blue-colored trace. Scale bar = 100 μ m. (G) Relative inner ear size in 60 hpf larvae of the indicated group. $n = 8-19$. *, $P < 0.05$.

resulted in a similar reduction in the relative eye size as Igfbp2a. Finally, myrAkt, a constitutively active form of Akt, was introduced into the developing lens to test if the effect of Igfbp was via the Igf1r-mediated signaling pathway. As expected, co-expression of myrAkt with the Igfbp2a restored normal eye size (Fig. 2D). Likewise, co-expression of myrAkt also abolished the dnIgf1r-induced reduction in eye size

(Fig. 2D).

3.3. Targeted expression of Igfbps in the heart and inner ear reduces their relative growth

The above mentioned results suggest that local Igf signaling is critical

in regulating eye size and its allometric scaling. To determine that Igf signaling also regulates other organ size, we used the *cmlc2* promoter to drive transgene expression in the developing heart and the *omp1* promoter in the otic vesicles (inner ears) transiently (Supplemental Fig. S1C and D). The heart-specific YFP expression and inner ear-specific expression of GFP were confirmed (Fig. 3A and D, E). The effect of *Igfbp2a* expression on heart growth was measured by MF20 antibody staining (Fig. 3B). The relative heart size in the *Igfbp2a* group was significantly smaller than that of the control groups ($77.7 \pm 2.90\%$, $P < 0.05$, Fig. 3C). Expression of *Igfbp5b* resulted in a significant decrease of the relative inner ear size ($83.4 \pm 2.84\%$, $P < 0.05$, Fig. 3F and G). These results suggest local Igf signaling is critical in regulating the heart and inner ear growth and their allometric scaling.

These findings suggest that local Igf availability and biological activity plays an important role in determining the organ size and allometric scaling. This is not limited to the eye because perturbing local Igf signaling in the heart and inner ear had similar effect. Our findings in zebrafish are also in line with previous discoveries made in the mouse model. Genetic deletion of IGF-1 specifically in the liver resulted in an 80% reduction in circulating endocrine IGF-1 but it did not change body size (Yakar et al., 1999). IGFBP-2 knockout male mice did not affect the body size but altered spleen and liver size (Wood et al., 2000).

An intriguing paradox in IGFBP biology is that while overexpression or addition of exogenous IGFBPs inhibits or potentiates IGF actions or even has IGF-independent actions *in vitro* and *in vivo*, IGFBP/Igfbp knockout mutant mice or zebrafish often do not exhibit major phenotypes (Allard and Duan, 2018; Hoeflich et al., 2018). One proposed explanation is genetic redundancy and compensation. Compensation by paralogous genes, caused by the upregulation of a family member with similar function in response to gene loss, has been reported in mouse, worm, zebrafish, and other model organisms (Jakutis and Stainier, 2021). Indeed, levels of IGFBPs-1, -3, and -4 were all elevated in the IGFBP-2 knockout mice (Wood et al., 2000). Another emerging explanation is genetic robustness (Jakutis and Stainier, 2021). Genetic robustness refers to the invariance of the phenotype in the face of genetic perturbations. A classic and naturally occurred example is sex chromosome dosage compensation. Recent studies using CRISPR have found major discrepancies in phenotypes between permanent knockout and transient knockdowns. When zebrafish IGFBP-3 was deleted, for example, no phenotypes were detected. However, when zebrafish IGFBP-3 was knocked down using antisense morpholinos, it resulted in defects in the development of the pharyngeal skeleton and inner ear (Allard and Duan, 2018; Li et al., 2005). In addition, recent studies showed that different IGFBPs may be involved in the regulation of local IGF signaling under aberrant conditions. One example is the role of *Igfbp5a* in regulating low calcium stress-induced ionocyte proliferation (Liu et al., 2018). In zebrafish, *igfbp5a* is specifically and highly expressed in Ca^{2+} transporting ionocytes, known as NaR cells (Dai et al., 2014). Under low calcium stress condition, these ionocytes rapidly proliferate to allow increased calcium import. This is considered to be an adaptive response allowing fish to acquire calcium for survival under low calcium stress. This elevated ionocyte proliferation is blunted in *igfbp5a* knockout fish. As a result, *igfbp5a* knockout fish, but not their siblings, die rapidly under low calcium stress (Liu et al., 2018). When raised in calcium-rich media, however, these mutant fish are indistinguishable from their wild type siblings (Liu et al., 2018). Another example is the role of *Igfbp1* in responding to catabolic conditions (hypoxia, starvation, stress etc.) by slowing down embryo growth and developmental rate in order to conserve scarce resources (Kajimura et al., 2005; Kajimura and Duan, 2007). Clearly, more studies are needed to understand the intricate interplays among different IGFBPs/IGFBPs and the specific physiological/pathological conditions involved.

4. Conclusion remarks

Nearly a century ago, Harrison performed organ transplant

experiments in salamanders to determine the importance of organ-intrinsic (autonomous) vs. extrinsic (non-autonomous) mechanisms in organ size control (Harrison, 1924). When transplanted a limb from an embryo of a large size salamander species into a small size salamander species, the limb grows up to the size of the donor animal and *vice versa*. This classic study clearly demonstrated the importance of the organ-intrinsic mechanism in organ size control and allometric scaling. The findings made in the present studies, together with previous studies in insect models (Mirth and Shingleton, 2012; Texada et al., 2020), suggest that local IGF/ILP availability and activity may be a part of the intrinsic organ size control mechanism.

CRediT authorship contribution statement

Hiroyasu Kamei: Conceptualization, Methodology, Formal analysis, Investigation, Writing – original draft, Writing – review & editing, Visualization, Project administration, Funding acquisition. **Cunning Duan:** Conceptualization, Methodology, Investigation, Resources, Writing – original draft, Writing – review & editing, Supervision, Project administration, Funding acquisition.

Declaration of Competing Interest

The authors declare that they have no known competing financial interests or personal relationships that could have appeared to influence the work reported in this paper.

Acknowledgement

We are grateful to Dr. Sumiko Watanabe, The University of Tokyo, for providing the α Cry promoter DNA.

Funding

This work was supported by NSF grant IOS-1557850 and IOS-1755268 to CD, the Japan Society for the Promotion of Science, Oversea Postdoctoral Research Fellow program (20-475), and Japan Society for the Promotion of Science, Grant-in-Aid for Scientific Research (C) (18K06014) to HK. The funders had no role in study design, data collection and analysis, decision to publish, or manuscript preparation.

Appendix A. Supplementary data

Supplementary data to this article can be found online at <https://doi.org/10.1016/j.ygcen.2021.113922>.

References

- Allard, J.B., Duan, C., 2018. IGF-binding proteins: why do they exist and why are there so many? *Front. Endocrinol. (Lausanne)* 9, 117.
- Clemmons, D.R., 2012. Metabolic actions of insulin-like growth factor-I in normal physiology and diabetes. *Endocrinol. Metab. Clin. N. Am.* 41 (2), 425–443 vii–viii.
- Clemmons, D.R., 2016. Role of IGF binding proteins in regulating metabolism. *Trends Endocrinol. Metab.* 27 (6), 375–391.
- Dai, W., Kamei, H., Zhao, Y., Ding, J., Du, Z., Duan, C., 2010. Duplicated zebrafish insulin-like growth factor binding protein-5 genes with split functional domains: evidence for evolutionarily conserved IGF binding, nuclear localization, and transactivation activity. *FASEB J.* 24 (6), 2020–2029.
- Dai, W., Bai, Y., Hebda, L., Zhong, X., Liu, J., Kao, J., Duan, C., 2014. Calcium deficiency-induced and TRP channel-regulated IGF1R-PI3K-Akt signaling regulates abnormal epithelial cell proliferation. *Cell Death Differ.* 21 (4), 568–581.
- Duan, C., Allard, J.B., 2020. Insulin-like growth factor binding protein-5 in physiology and disease. *Front. Endocrinol. (Lausanne)* 11, 100.
- Duan, C., Ding, J., Li, Q., Tsai, W., Pozios, K., 1999. Insulin-like growth factor binding protein 2 is a growth inhibitory protein conserved in zebrafish. *Proc. Natl. Acad. Sci. U.S.A.* 96 (26), 15274–15279.
- Duan, C., Ren, H., Gao, S., 2010. Insulin-like growth factors (IGFs), IGF receptors, and IGF-binding proteins: roles in skeletal muscle growth and differentiation. *Gen. Comp. Endocrinol.* 167 (3), 344–351.
- Duan, C., Xu, Q., 2005. Roles of insulin-like growth factor (IGF) binding proteins in regulating IGF actions. *Gen. Compos. Endocrinol.* 142 (1–2), 44–52.

Emlen, D.J., Warren, I.A., Johns, A., Dworkin, I., Lavine, L.C., 2012. A mechanism of extreme growth and reliable signaling in sexually selected ornaments and weapons. *Science* 337 (6096), 860–864.

Firth, S.M., Baxter, R.C., 2002. Cellular actions of the insulin-like growth factor binding proteins. *Endocr. Rev.* 23 (6), 824–854.

Frankino, W.A., Bakota, E., Dworkin, I., Wilkinson, G.S., Wolf, J.B., Shingleton, A.W., 2019. Individual cryptic scaling relationships and the evolution of animal form. *Integr. Comp. Biol.* 59 (5), 1411–1428.

Harrison, R.G., 1924. Some unexpected results of the heteroplastic transplantation of limbs. *Proc. Natl. Acad. Sci. U.S.A.* 10 (2), 69–74.

Hoeflich, A., Pintar, J., Forbes, B., 2018. Editorial: current perspectives on insulin-like growth factor binding protein (IGFBP) research. *Front. Endocrinol. (Lausanne)* 9, 667.

Huang, C.J., Tu, C.T., Hsiao, C.D., Hsieh, F.J., Tsai, H.J., 2003. Germ-line transmission of a myocardium-specific GFP transgene reveals critical regulatory elements in the cardiac myosin light chain 2 promoter of zebrafish. *Dev. Dynam.* 228 (1), 30–40.

Jakutis, G., Stainier, D.Y.R., 2021. Genotype-phenotype relationships in the context of transcriptional adaptation and genetic robustness. *Annu. Rev. Genet.*

Kajimura, S., Duan, C., 2007. Insulin-like growth factor-binding protein-1: an evolutionarily conserved fine tuner of insulin-like growth factor action under catabolic and stressful conditions. *J. Fish Biol.* 71, 309–325.

Kajimura, S., Aida, K., Duan, C., 2005. Insulin-like growth factor-binding protein-1 (IGFBP-1) mediates hypoxia-induced embryonic growth and developmental retardation. *Proc. Natl. Acad. Sci. U.S.A.* 102 (4), 1240–1245.

Kamei, H., Lu, L., Jiao, S., Li, Y., Gyurup, C., Laursen, L.S., Osvig, C., Zhou, J., Duan, C., 2008. Duplication and diversification of the hypoxia-inducible IGFBP-1 gene in zebrafish. *PLoS ONE* 3 (8), e3091.

Kamei, H., Ding, Y., Kajimura, S., Wells, M., Chiang, P., Duan, C., 2011. Role of IGF signaling in catch-up growth and accelerated temporal development in zebrafish embryos in response to oxygen availability. *Development* 138 (4), 777–786.

Kawakami, K., 2004. Transgenesis and gene trap methods in zebrafish by using the Tol2 transposable element. *Methods Cell Biol.* 77, 201–222.

Kimmel, C.B., Ballard, W.W., Kimmel, S.R., Ullmann, B., Schilling, T.F., 1995. Stages of embryonic development of the zebrafish. *Dev. Dyn.* 203 (3), 253–310.

Kurita, R., Sagara, H., Aoki, Y., Link, B.A., Arai, K., Watanabe, S., 2003. Suppression of lens growth by alpha A-crystallin promoter-driven expression of diphtheria toxin results in disruption of retinal cell organization in zebrafish. *Dev. Biol.* 255 (1), 113–127.

Li, Y., Xiang, J., Duan, C., 2005. Insulin-like growth factor-binding protein-3 plays an important role in regulating pharyngeal skeleton and inner ear formation and differentiation. *J. Biol. Chem.* 280 (5), 3613–3620.

Liu, C., Xin, Y., Bai, Y., Lewin, G., He, G., Mai, K., Duan, C., 2018. Ca(2+) concentration-dependent premature death of igfbp5a(-/-) fish reveals a critical role of IGF signaling in adaptive epithelial growth. *Sci. Signal.* 11 (548).

Lu, C., Lam, H.N., Menon, R.K., 2005. New members of the insulin family: regulators of metabolism, growth and now reproduction. *Pediatr. Res.* 57 (5 Pt 2), 70R–73R.

Maures, T.J., Duan, C., 2002. Structure, developmental expression, and physiological regulation of zebrafish IGF binding protein-1. *Endocrinology* 143 (7), 2722–2731.

Mirth, C.K., Shingleton, A.W., 2012. Integrating body and organ size in *Drosophila*: recent advances and outstanding problems. *Front. Endocrinol. (Lausanne)* 3, 49.

Mirth, C.K., Anthony Frankino, W., Shingleton, A.W., 2016. Allometry and size control: what can studies of body size regulation teach us about the evolution of morphological scaling relationships? *Curr. Opin. Insect Sci.* 13, 93–98.

Onuma, T.A., Ding, Y., Abraham, E., Zohar, Y., Ando, H., Duan, C., 2011. Regulation of temporal and spatial organization of newborn GnRH neurons by IGF signaling in zebrafish. *J. Neurosci.* 31 (33), 11814–11824.

Shingleton, A.W., Das, J., Vinicius, L., Stern, D.L., 2005. The temporal requirements for insulin signaling during development in *Drosophila*. *PLoS Biol.* 3 (9), e289.

Tang, H.Y., Smith-Caldas, M.S., Driscoll, M.V., Salhadar, S., Shingleton, A.W., 2011. FOXO regulates organ-specific phenotypic plasticity in *Drosophila*. *PLoS Genet.* 7 (11), e1002373.

Texada, M.J., Koyama, T., Rewitz, K., 2020. Regulation of body size and growth control. *Genetics* 216 (2), 269–313.

Vea, I.M., Shingleton, A.W., 2020. Network-regulated organ allometry: The developmental regulation of morphological scaling. *Wiley Interdiscip. Rev. Dev. Biol.* e391.

Wang, X., Lu, L., Li, Y., Li, M., Chen, C., Feng, Q., Zhang, C., Duan, C., 2009. Molecular and functional characterization of two distinct IGF binding protein-6 genes in zebrafish. *Am. J. Physiol. Regul. Integr. Comp. Physiol.* 296 (5), R1348–R1357.

Wood, A.W., Duan, C., Bern, H.A., 2005a. Insulin-like growth factor signaling in fish. *Int. Rev. Cytol.* 243, 215–285.

Wood, T.L., Rogler, L.E., Czick, M.E., Schuller, A.G., Pintar, J.E., 2000. Selective alterations in organ sizes in mice with a targeted disruption of the insulin-like growth factor binding protein-2 gene. *Mol. Endocrinol.* 14 (9), 1472–1482.

Wood, A.W., Schlueter, P.J., Duan, C., 2005b. Targeted knockdown of insulin-like growth factor binding protein-2 disrupts cardiovascular development in zebrafish embryos. *Mol. Endocrinol.* 19 (4), 1024–1034.

Yakar, S., Liu, J.L., Stannard, B., Butler, A., Accili, D., Sauer, B., LeRoith, D., 1999. Normal growth and development in the absence of hepatic insulin-like growth factor I. *Proc. Natl. Acad. Sci. U.S.A.* 96 (13), 7324–7329.

Zhong, Y., Lu, L., Zhou, J., Li, Y., Liu, Y., Clemmons, D.R., Duan, C., 2011. IGF binding protein 3 exerts its ligand-independent action by antagonizing BMP in zebrafish embryos. *J. Cell Sci.* 124 (Pt 11), 1925–1935.

Zhou, J., Li, W., Kamei, H., Duan, C., 2008. Duplication of the IGFBP-2 gene in teleost fish: protein structure and functionality conservation and gene expression divergence. *PLoS ONE* 3 (12), e3926.